



Influence of climate variability, fire and phosphorus limitation on vegetation structure and dynamics of the Amazon–Cerrado border

Emily Ane Dionizio¹, Marcos Heil Costa¹, Andrea D. de Almeida Castanho², Gabrielle Ferreira Pires¹, Beatriz Schwantes Marimon³, Ben Hur Marimon-Junior³, Eddie Lenza³, Fernando Martins Pimenta¹, Xiaojuan Yang⁴, and Atul K. Jain⁵

¹Department of Agricultural Engineering, Federal University of Viçosa (UFV), Viçosa, MG 36570-000, Brazil

²The Woods Hole Research Center, 149 Woods Hole Rd., Falmouth, MA 02540, USA

³Plant Ecology Laboratory, State University of Mato Grosso, Nova Xavantina Campus, Nova Xavantina, MT 78690-000, Brazil

⁴Environmental Sciences Division and Climate Change Science Institute, Oak Ridge National Laboratory, Oak Ridge, TN 37831, USA

⁵Department of Atmospheric Sciences, University of Illinois at Urbana-Champaign, Urbana, IL 61801, USA

Correspondence: Emily Ane Dionizio (emilyy.ane@gmail.com)

Received: 19 April 2017 – Discussion started: 12 May 2017

Revised: 2 January 2018 – Accepted: 3 January 2018 – Published: 15 February 2018

Abstract. Climate, fire and soil nutrient limitation are important elements that affect vegetation dynamics in areas of the forest–savanna transition. In this paper, we use the dynamic vegetation model INLAND to evaluate the influence of interannual climate variability, fire and phosphorus (P) limitation on Amazon–Cerrado transitional vegetation structure and dynamics. We assess how each environmental factor affects net primary production, leaf area index and above-ground biomass (AGB), and compare the AGB simulations to an observed AGB map. We used two climate data sets (monthly average climate for 1961–1990 and interannual climate variability for 1948–2008), two data sets of total soil P content (one based on regional field measurements and one based on global data), and the INLAND fire module. Our results show that the inclusion of interannual climate variability, P limitation and fire occurrence each contribute to simulating vegetation types that more closely match observations. These effects are spatially heterogeneous and synergistic. In terms of magnitude, the effect of fire is strongest and is the main driver of vegetation changes along the transition. Phosphorus limitation, in turn, has a stronger effect on transitional ecosystem dynamics than interannual climate variability does. Overall, INLAND typically simulates more than 80 % of the AGB variability in the transition zone. However, the AGB in many places is clearly not well simulated,

indicating that important soil and physiological factors in the Amazon–Cerrado border region, such as lithology, water table depth, carbon allocation strategies and mortality rates, still need to be included in the model.

1 Introduction

The Amazon and the Cerrado are the two largest and most important phytogeographical domains in South America. The Amazon forest has been globally recognized not only for its species diversity and richness but also because it plays important roles in the global climate by regulating water (Bonan, 2008; Pires and Costa, 2013) and heat fluxes (Shukla et al., 1990; Roy and Avissar, 2002; da Rocha et al., 2004). The Cerrado is recognized as the most species-rich savanna in the world (Myers et al., 2000; Klink and Machado, 2005). It is characterized by landscapes ranging from sparse fields to dense woodlands, which may mix with Amazon rainforest vegetation in transitional areas. The Amazon–Cerrado transition extends 6270 km from northeast to southwest in Brazil, and ecotonal vegetation around this transition includes a mix of tropical forest and savanna species (Torello-Raventos et al., 2013).

Gradients of seasonal rainfall, water deficit, fire occurrence, herbivory and soil fertility have been reported as the main factors that characterize transitions between forest and savanna globally (Lehmann et al., 2011; Hoffman et al., 2012; Murphy and Bowman, 2012). However, few studies have evaluated the individual and combined effects of these factors on Brazilian ecotones (Marimon-Junior and Haridasan, 2005; Elias et al., 2013; Vourtilis et al., 2013).

It is challenging to assess the degree of interaction among these environmental factors in the transitional region and to infer how each one influences the distribution of the regional vegetation. In this case, dynamic global vegetation models (DGVMs) can be powerful tools to isolate the influences of climate, fire and nutrients, thereby helping to understand their large-scale effects on vegetation (House et al., 2003; Favier et al., 2004; Hirota et al., 2010; Hoffman et al., 2012).

Previous modeling studies using DGVMs that investigated climate effects in the Amazon indicate that the rainforest could experience changes in rainfall patterns that would transform the forest into either an ecosystem with sparser vegetation, similar to a savanna, – what has been called the “savannization of the Amazon” (Shukla et al., 1990; Cox et al., 2000, 2004; Oyama and Nobre, 2003; Betts et al., 2004; Salazar et al., 2007) – or into a seasonal forest (Malhi et al., 2009; Pereira et al., 2012; Pires and Costa, 2013). These studies have had great importance for the improvement of terrestrial biosphere modeling, but they neglect two important processes in tropical ecosystem dynamics: fire occurrence and nutrient limitation, particularly phosphorus (P) limitation.

In tropical ecosystems, fire plays an important ecological role and influences the productivity, biogeochemical cycles, and vegetation dynamics of transitional biomes, not only by changing the phenology and physiology of plants but also by modifying competition among trees and lower canopy plants such as grasses, shrubs and lianas. Fire occurrence, depending on its frequency and intensity, may increase the mortality of trees and transform an undisturbed forest into a disturbed and flammable one (House et al., 2003; Hirota et al., 2010; Hoffmann et al., 2012). Fires also affect the dynamics of nutrients in savanna ecosystems, mainly by changing the N : P relationship and P availability in the soil (Nardoto et al., 2006).

Studies suggest that P is the main limiting nutrient within tropical forests (Malhi et al., 2009; Mercado et al., 2011; Quesada et al., 2012), unlike in temperate forests, where nitrogen (N) is the main nutrient that limits productivity. Phosphorus is easily bound by soil minerals due to the large amount of iron and aluminum oxides in the acidic and strongly weathered soils of the Amazon and the Cerrado (Dajoz, 2005; Goedert, 1986). In the tropics, the warm and wet climate favors high biological activity in the soil and rapid litter decomposition, therefore nitrogen is not generally limiting for plant fixation. In the Cerrado, higher soil fertility is related to regions with greater woody plant abundance and

less grass cover, similar to conditions found in the Amazon rainforest (Moreno et al., 2008; Vourtilis et al., 2013; Veenendaal et al., 2015). However, phosphorus limitation is often neglected by DGVMs, which usually assume unlimited P availability and consider N to be the main limiting nutrient. Although N does affect tree growth (Davidson et al., 2004), it is not a limiting tropical soil nutrient when compared to total P availability, which affects competition between trees.

In principle, in transitional forests, where the climate is intermediate between wet and seasonally dry, the heterogeneous structure and phenology make it difficult to represent these forests in models. The Amazon–Cerrado border is the result of the expansion and contraction of the Cerrado into the forest (see Marimon et al., 2006; Morandi et al., 2016), especially in Mato Grosso state where extreme events, such as intense droughts, influence the vegetation dynamics (Marimon et al., 2014) and the nutrient (Oliveira et al., 2017) and carbon cycling (Valadão et al., 2016).

Currently, no model has been able to accurately simulate the vegetation transition between the Amazon and the Cerrado. In general DGVMs simulate evergreen forest along the Amazon–Cerrado border and miss savanna occurrence (Botta and Foley, 2002; Bond et al., 2005; Salazar et al., 2007; Smith et al., 2014). This difficulty may be because these models neglect or poorly represent nutrient limitation, soil properties or disturbances such as fire. Thus, we need a better understanding of the controls on transitional vegetation in order to determine the appropriate model parameters and simulate relations between environmental factors and transitional vegetation physiognomies.

In this paper, we use the dynamic vegetation model IN-LAND (Integrated Model of Land Surface Processes) to evaluate the influence of interannual climate variability, fire occurrence and P limitation on Amazon–Cerrado transitional vegetation dynamics and structure. We assess how each element affects net primary production (NPP), leaf area index (LAI) and aboveground biomass (AGB) and compare the simulated AGB to observed AGB data. The results presented here are important for building models that accurately represent transitional vegetation and show the need for including the spatial variability in ecophysiological parameters for these areas.

2 Materials and methods

2.1 Study area

The present study focuses on the Amazon–Cerrado transition region (Fig. 1). We use the official delimitation of the Brazilian biomes proposed by IBGE (2004) and define five transects along the transition border with a $1^\circ \times 1^\circ$ grid size (the terms “transition”, “Amazon–Cerrado transition” and “forest–savanna transition” are used interchangeably throughout this manuscript). Transects 1 to 4 all span the Amazon–Cerrado border, extending approximately 330 km

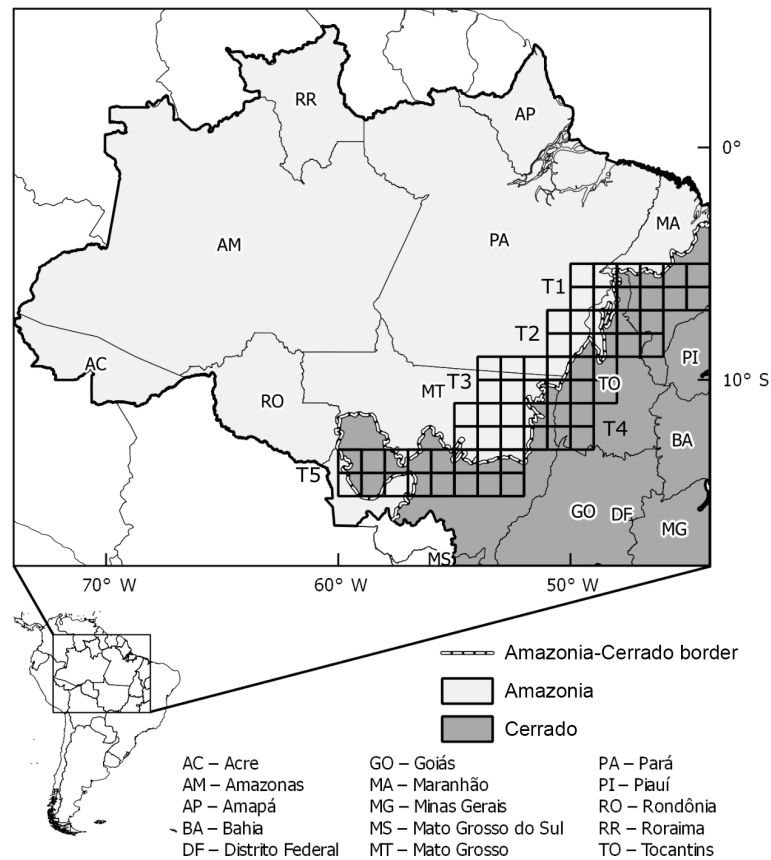


Figure 1. Delimitation of the study area, showing Amazonia (in light gray) and the Cerrado (in dark gray) (IBGE, 2004), and the location of five west–east transects used in this work (from T1 to T5). The dashed line represents the border between biomes.

into each biome, while Transect 5 is 880 km long and runs along the southern Amazon–Cerrado border. The transects are located as follows: Transect 1 (T1; 44–50° W, 5–7° S), Transect 2 (T2; 46–51° W, 7–9° S), Transect 3 (T3; 48–54° W, 9–11° S), Transect 4 (T4; 49–55° W, 11–13° S), and Transect 5 (T5; 52–60° W, 13–15° S) (Fig. 1).

2.2 Description of the INLAND surface model

The Integrated Model of Land Surface Processes (INLAND) is the land-surface component of the Brazilian Earth System Model (BESM). INLAND, a revision of the IBIS model (Integrated Biosphere Simulator, described by Foley et al., 1996; Kucharik et al., 2000), has been developed by assembling and standardizing different IBIS versions and adding improvements in software engineering. We used the version described by Senna et al. (2009) as the starting point for INLAND without changes in tuning, aside from the addition of the P parameterization described below. Code is available from <http://www.biosfera.dea.ufv.br/en-US/download-inland>.

The model considers changes in the composition and structure of vegetation in response to the environment and incorporates important aspects of biosphere–atmosphere in-

teractions. The model simulates the exchanges of energy, water, carbon and momentum between soil, vegetation and atmosphere. These processes are organized in a hierarchical framework and operate at different time steps, ranging from 60 min to 1 year, coupling ecological, biophysical and physiological processes. The vegetation composition is represented by 12 plant functional types (PFTs; e.g., tropical broadleaf evergreen trees or C₄ grasses), and the vegetation structure is represented by two canopy layers: upper (arboreal PFTs) and lower (shrubs and grasses, but no arboreal PFTs). The photosynthesis and respiration processes are simulated in a mechanistic manner using the Ball–Berry–Farquhar model (details in Foley et al., 1996). The vegetation phenology module simulates processes such as budding and senescence based on a drought phenology scheme for tropical deciduous trees. The dynamic vegetation module computes the following variables yearly for each PFT: gross and net primary productivity (GPP and NPP), changes in AGB pools, simple mortality disturbance processes and resultant LAI; this allows vegetation type and cover to change with time. The partitioning of the NPP for each PFT resolves carbon into three AGB pools: leaves, stems and fine roots. The LAI of each PFT is obtained simply by dividing leaf carbon

by specific leaf area, which in INLAND is considered fixed (one value) for each PFT.

INLAND has eight soil layers to simulate the diurnal and seasonal variations of heat and moisture. Each layer is described in terms of soil temperature, volumetric water content and ice content (Thompson and Pollard, 1995; Foley et al., 1996). Furthermore, all of these processes are influenced by soil texture and amount of organic matter within the soil profile.

Using these aspects of vegetation dynamics and soil physical properties, the model can simulate plant competition for light and water between trees, shrubs and grasses through shading and differences in water uptake (Foley et al., 1996). These PFTs can coexist within a grid cell, and their annual LAI values indicate the dominant vegetation type within a grid cell. For example, the dominant vegetation type is Tropical Evergreen Forest if the tropical broadleaf evergreen tree PFT has an annual mean upper canopy LAI (LAI_{upper}) above $2.5 \text{ m}^2 \text{ m}^{-2}$. On the other hand, the dominant vegetation type is Tropical Deciduous Forest if the tropical broadleaf drought-deciduous tree PFT has an annual mean LAI_{upper} above $2.5 \text{ m}^2 \text{ m}^{-2}$. Where total tree LAI (LAI_{upper}) is between 0.8 and $2.5 \text{ m}^2 \text{ m}^{-2}$, the dominant vegetation type is Savanna, and LAI_{upper} values smaller than $0.8 \text{ m}^2 \text{ m}^{-2}$ represent a Grassland vegetation type.

We assume that the vegetation types Tropical Evergreen Forest and Tropical Deciduous Forest in INLAND represent the Amazon rainforest, while Savanna and Grassland represent the Cerrado. INLAND's Savannas would be equivalent to the Cerrado physiognomies *Cerradão* and *Cerrado sensu strictu*, while INLAND's Grasslands would be equivalent to the physiognomies *Campo sujo* and *Campo Limpo* (sensu Ribeiro and Walter, 2008).

Soil chemical properties are represented by carbon (C), nitrogen (N) and phosphorus (P). The carbon cycle is simulated through vegetation, litter and soil organic matter, where the biogeochemical module is similar to the CENTURY model (Verberne et al., 1990; Parton et al., 1993). The amount of C existing in the first meter of soil is divided into different compartments characterized by their residence time, which can vary from just hours for microbial AGB and organic matter to several years for lignin. The model considers only soil N transformations and C decomposition, but the N cycle is not fully simulated, and N does not influence the vegetation productivity, i.e., there is a fixed C : N ratio. The P cycle is also not fully implemented; instead, P limitation is spatially parameterized through the linear relationship developed by Castanho et al. (2013) to limit the gross primary productivity. A map of total phosphorus in the soil (P_{total}) is used by the model to estimate the maximum capacity of carboxylation by the Rubisco enzyme (V_{max}) for each grid cell using Eq. (1):

$$V_{max} = 0.1013 P_{total} + 30.037, \quad (1)$$

where V_{max} and P_{total} are given in $\mu\text{mol CO}_2 \text{ m}^{-2} \text{ s}^{-1}$ and mg P kg^{-1} soil, respectively. This equation has been based on data for tropical evergreen and deciduous trees and is applied only to these two PFTs; the other PFTs are unaffected.

INLAND also contains a spatial fire module, based on the Canadian Terrestrial Ecosystem Model CTEM (Arora and Boer, 2005). In this module, three aspects of the fire triangle are considered: the availability of fuel to burn, the flammability of vegetation and the presence of an ignition source. Each is represented daily by an independently calculated probability, and the product of the three is the probability of fire occurrence, calculated daily. Availability of fuel to burn depends on biomass, flammability depends on soil moisture, and ignition depends on a random lightning occurrence and a constant anthropogenic ignition probability. The daily fire occurrence probability is equal to the daily AGB burned fraction. The AGB burned fraction is accumulated throughout the year, and its ratio is applied at the end of each year to the grid cell area, reducing the leaf, wood and root biomass pools. After fire occurrence, the carbon allocation and mortality rates are not modified, and the recovery of vegetation dynamics from a fire follows the model standard procedure, where upper and lower LAI are decreased, triggering competition between both canopies for light.

2.3 Observed data

2.3.1 Phosphorus databases

We used two P databases to estimate V_{max} (Eq. 1): one regional (referred to as PR) and one global (referred to as PG). In addition, a control P map (PC) represents the unlimited nutrient availability case, equivalent to a V_{max} of $65 \mu\text{mol CO}_2 \text{ m}^{-2} \text{ s}^{-1}$, or 350 mg P kg^{-1} soil, according to Eq. (1).

The PR database was developed using data on total P in the soil for the Amazon basin published by Quesada et al. (2010), plus 54 additional samples measuring available P (P extracted via Mehlich-1 extraction, $P_{Mehlich-1}$ (Fig. 2a)). We used the $P_{Mehlich-1}$ values and clay contents measured in a forest–savanna transition region in Brazil (Mato Grosso state) to estimate P_{total} and expand the coverage area of the P data (Sect. S1 in the Supplement). These 54 samples were gridded to a $1^\circ \times 1^\circ$ grid to be compatible with the spatial resolution used by INLAND, resulting in 12 additional pixels with observed total P content (Fig. 2a). For pixels without observed P_{total} , the P_{total} was assumed to be 350 mg P kg^{-1} soil, similar to the PC conditions.

A global data set of P_{total} (PG; Fig. 2b) was also used to estimate V_{max} . This global data set is part of a database containing six global maps of the different forms of P in the soil (Yang et al., 2013). The uncertainties and limitations associated with this database are restricted to the Hedley fractionation data used, which are 17 % for slightly weathered soils, 65 % for soils at an intermediate stage of weathering and 68 % for highly weathered soils (Yang et al., 2013).

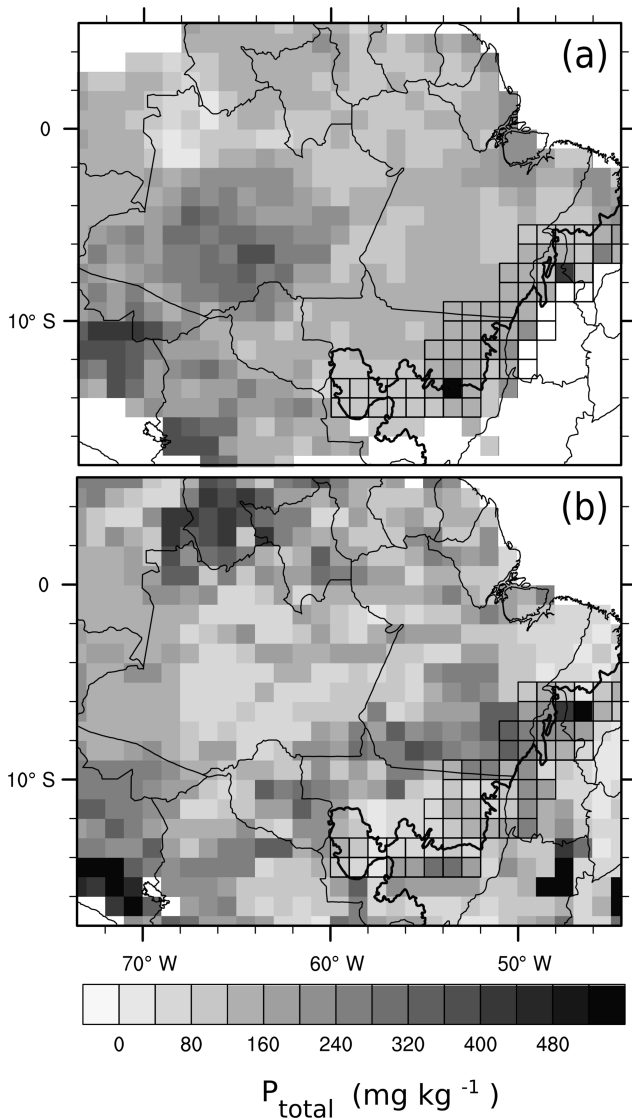


Figure 2. (a) Regional map of total P in the soil (PR) and (b) global map of total P in the soil (PG; Yang et al., 2013).

2.3.2 Aboveground biomass (AGB) database

The AGB database used was created by Nogueira et al. (2015) and considered undisturbed (pre-deforestation) vegetation existing in the Brazilian Amazon. This database was compiled from a vegetation map on a scale of 1 : 250000 (IBGE, 1992) and AGB averages from 41 published studies that conducted direct sampling in either forest (2317 plots) or non-forest or contact zones (1830 plots). We bilinearly interpolated the AGB (dry weight) for each transect to a resolution of $1^\circ \times 1^\circ$ to ensure compatibility of the observed and simulated data.

Five longitudinal transects (Fig. 1) were individually used to characterize AGB at the Amazon–Cerrado border (Fig. 3a, b). For T1, T2, T3 and T4, the higher AGB values in

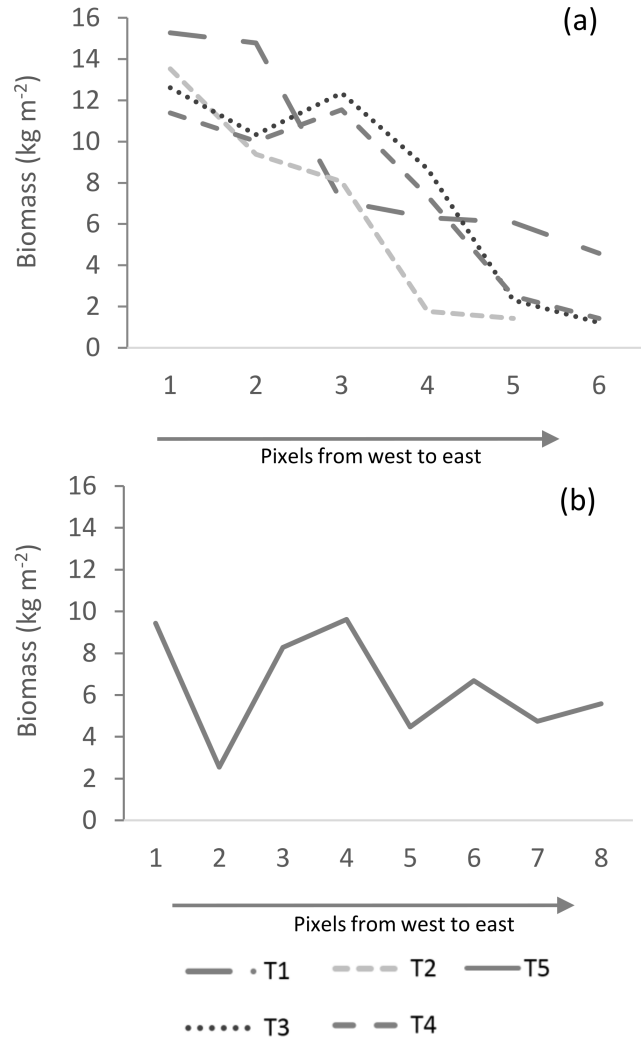


Figure 3. Average variations in aboveground biomass (AGB) in pixels from west to east in the Amazon–Cerrado transition for transects (a) T1, T2, T3 and T4, and (b) T5.

the west and lower values in the east are consistent with the transition from a dense and woody vegetation (the Amazon forest) towards a sparse vegetation with lower AGB (the Cerrado). However, T1 shows a more gradual reduction of AGB along the west to east gradient, while for T2, T3 and T4 the transition is more abrupt. For T5, there is no west–east gradient; AGB heterogeneity is high, and low AGB predominates across the transect (Fig. 3b).

2.4 Simulations

The model was forced with prescribed climate data based on the Climate Research Unit (CRU) database (Harris et al., 2014). Two climate boundary conditions were used: the first is referred to as the monthly climatological average (CA) that represents the average climate for the period 1961–1990. The second climate boundary condition is the historical data

Table 1. Twelve simulation treatments evaluated by the INLAND model for the Amazon–Cerrado transition zone. CA, monthly climatological average, 1961–1990. CV, monthly climate data, 1948–2008. Nutrient limitation on V_{\max} : PC, no P limitation ($V_{\max} = 65 \mu\text{mol CO}_2 \text{ m}^{-2} \text{ s}^{-1}$); PR, regional P limitation; PG, global P limitation.

Climate	CO ₂	Fire (F)	V_{\max}		
			PC	PR	PG
CA	variable	off	CA + PC	CA + PR	CA + PG
CA	variable	on	CA + PC + F	CA + PR + F	CA + PG + F
CV	variable	off	CV + PC	CV + PR	CV + PG
CV	variable	on	CV + PC + F	CV + PR + F	CV + PG + F

Table 2. Individual and combined effects for each simulation treatment for the Amazon–Cerrado transition zone. CA, monthly climatological average, 1961–1990. CV, monthly climate data, 1948–2008. Nutrient limitation on V_{\max} : PC, no P limitation ($V_{\max} = 65 \mu\text{mol CO}_2 \text{ m}^{-2} \text{ s}^{-1}$); PR, regional P limitation; PG, global P limitation.

Climate (C)	Phosphorus (P)	Fire (F)
(CV + PC)–(CA + PC)	(CA + PR)–(CA + PC)	(CA + PC + F)–(CA + PC)
(CV + PR)–(CA + PR)	(CV + PR)–(CV + PC)	(CV + PC + F)–(CV + PC)
(CV + PG)–(CA + PG)	(CA + PG)–(CA + PC)	(CA + PR + F)–(CA + PR)
	(CV + PG)–(CV + PC)	(CV + PR + F)–(CV + PR)
		(CA + PG + F)–(CA + PG)
		(CV + PG + F)–(CV + PG)

set for the continuous period between 1948 and 2008, which provides information on interannual climate variability (CV). For both boundary conditions, the variables used are rainfall, solar radiation, wind velocity and maximum and minimum temperatures. The CRU database is developed from observations at meteorological stations across the world's land areas; it has been widely used by the scientific community in case studies to evaluate El Niño–Southern Oscillation (ENSO) effects and other modes of interannual climate variability (Foley et al., 2002; Marengo, 2004; Wang et al., 2014) because these data preserve the spatial mean of rainfall data, although they do not provide adequate representation of precipitation variance (Beguiría et al., 2016). The data set has a 1° spatial resolution and a monthly time resolution.

Soil texture data is based on the International Geosphere-Biosphere Programme – Data and Information System global IGBP-DIS (Hansen and Reed, 2000). In the CV group of runs, the model was spun-up by cycling the 1948–2008 climate data (a 61-year data set) seven times, totaling 427 years. In the CA group of runs, the annual mean climate data was cycled 427 times. In both cases, CO₂ varied from 278 to 380 ppmv, according to observations in the period, updated annually. In both cases, only the model results of the last 10 years were used to analyze the results.

The experimental design is a factorial combination of (1) the two climate scenarios (CA, monthly climatological average, 1961–1990; CV, monthly climate time series, 1948–2008), (2) the three scenarios for P limitation on V_{\max} (PC, no P limitation ($V_{\max} = 65 \mu\text{mol CO}_2 \text{ m}^{-2} \text{ s}^{-1}$); PR, regional P limitation; PG, global P limitation), and (3) the scenarios

including or excluding fire (F; Table 1). The 12 combinations in Table 1 allow the evaluation of individual and combined effects of climate, soil chemistry and fire incidence on the variables NPP, tree AGB, and LAI of the upper and lower canopies ($\text{LAI}_{\text{upper}}$, $\text{LAI}_{\text{lower}}$).

We consider that the difference between the simulations (CV + PC) and (CA + PC) represents the isolated effect of interannual climate variability without P limitation. The same logic is applied to isolate other factors, fire and P limitation, in different climate scenarios. For example, the fire effect under average climate without P limitation case is calculated by the difference between CA + PC + F and CA + PC. Similarly, the isolated effect of fire under a climate scenario with interannual variability without the influence of P limitation is calculated by the difference between CV + PC + F and CV + PC. The different combinations of climate scenarios with and without fire effects and with and without P limitations are described in Table 2.

2.5 Statistical analysis and determination of the best model configuration

The statistical analysis is divided into four parts. First, we present maps of the isolated effects for all of the simulated area, calculated as the average of the last 10 years of simulated spatial patterns. The statistical significance of these isolated effects on NPP, LAI and tree biomass are determined using the t test with $p < 0.05$. The results are tested in each pixel, for all of the simulated domain ($n = 10$).

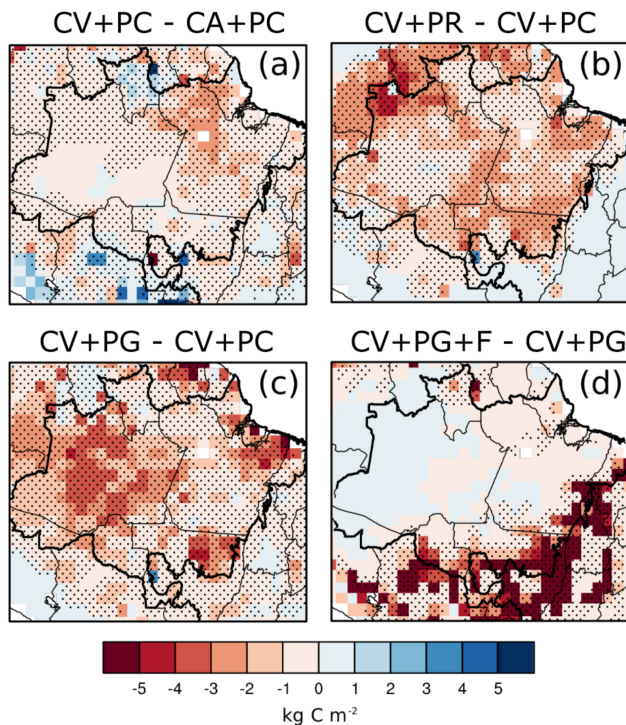


Figure 4. Effects of interannual climate variability (a), regional P limitation (b), global P limitation (c), and fire (d) on tree biomass (TB). The stippled areas indicate that the variables are significantly different compared to the control simulation at the level of 95 % according to the *t* test. The thick black line indicates the geographical limits of the biomes.

Second, we present an analysis of variance using one-way ANOVA and the Tukey–Kramer test in the transition zone. We consider all 31 pixels that fall in transects T1 to T5 (n_{pixels}). The results presented are based on the last 10 years of simulation (1999–2008, n_{years}) for the 12 combinations ($n_{\text{simulation}}$) in Table 1. We group the 12 treatments in three different ways in order to assess separately the effects of climate, P limitation, and fire. In Group 1 we group treatments according to climate treatment and compare results for all simulations that used CV versus those that used CA, regardless of P limitation or inclusion of fire (Group 1, $n = 1860$, ($n_{\text{pixel}} \times n_{\text{year}} \times (n_{\text{simulation}}/2)$). Similarly, in Group 2, to look at P limitation, we test if the PC, PR and PG scenarios differed significantly regardless of the fire or climate scenario used (Group 2, $n = 1240$, ($n_{\text{pixel}} \times n_{\text{year}} \times (n_{\text{simulation}}/3)$). In Group 3 we test if fire introduced a significant effect regardless of climate and P limitation scenario (Group 3, $n = 1860$, ($n_{\text{pixel}} \times n_{\text{year}} \times (n_{\text{simulation}}/2)$). Finally, all treatments are tested for each simulation in order to assess the individual and combined effects of climate, P limitation, and fire on NPP, LAI and AGB ($n_{\text{pixel}} \times n_{\text{year}} = 310$).

Third, a correlation coefficient between the simulated and observed values for AGB is calculated for each transect.

The simulated variables are averaged for the last 10 years of simulations (1999–2008) and compared to the AGB from Nogueira et al. (2015) within a grid cell.

Finally, we evaluate INLAND’s ability to assign the dominant vegetation type by analyzing 10 years of probability of occurrence. If the dominant vegetation type (evergreen tropical forest or deciduous forest for the Amazon rainforest, and savanna or grasslands for Cerrado) in a pixel is the same in more than 90 % of the simulated years (9 out of 10), then the simulated vegetation type is defined as “very robust” for that pixel; if it occurs in 70–90 % of the simulated years, the simulated result is considered to be “robust”. If the dominant vegetation occurred in less than 70 % of simulated years, the pixel is considered “transitional” vegetation.

3 Results

3.1 Influence of climate, fire and phosphorus on the Amazon–Cerrado transition region

3.1.1 Spatial patterns

Overall, the inclusion of interannual CV decreased the simulated average tree biomass (TB) by 3.8 % for the entire Brazilian Amazon, and by 8.7 % for the entire Cerrado in comparison to results obtained using CA, calculated as (CV + PC)–(CA + PC) (Fig. 4a). The spatial differences between CV and CA for TB simulations are statistically significant and range from -3 to $+2$ kg C m⁻². The state of Pará, with a higher influence of the El Niño phenomenon, experienced the largest decrease in TB in the CV simulation. In the state of Roraima, on the other hand, there was an increase of about 2 kg C m⁻² in TB when CV was considered. Bolivia and southwestern Mato Grosso state also presented, in some grid points, a significant increase in TB exceeding 2 kg C m⁻².

On average, P acts as a limiting factor on the simulated TB, decreasing it by 13 % in the regional P simulation (PR) and by 15 % in the global P simulation (PG). In PR, TB decreased mainly in southeastern Amazonia (between Pará and northeastern Mato Grosso states) and northwestern Amazonas state (Fig. 4b). In PG, the largest TB declines occurred in central Amazonia, northeastern Pará and northeastern Mato Grosso (Fig. 4c). In the Cerrado, on the other hand, TB declined by 2 % for PR and 9 % for PG with respect to the control simulation. In PR, the few pixels in the Cerrado that have P limitation showed a significant decrease in TB (Fig. 4b), while in PG the TB reduction was statistically significant for most of the Cerrado domain, except in southern Tocantins state (Fig. 4c).

The tree biomass reduction due to fire events is much higher in magnitude than the effect of P limitation or interannual climate variability (Fig. 4d). The small or null fire effect in the central Amazon rainforest is mainly related to that re-

Table 3. Summary of average NPP, LAI and AGB for the Amazon–Cerrado transition zone over the transect domains, considering all simulations with CA and CV, regardless of fire presence or P limitation. One-way ANOVA results are also shown, including F statistics and p values. Values within each column followed by a different letter differ significantly ($p < 0.05$) according to the Tukey–Kramer test ($n = 1860: 31 \text{ pixels} \times 10 \text{ years} \times n_{\text{simulation}}/2$).

Group 1	NPP	LAI _{total}	LAI _{lower}	LAI _{upper}	AGB
	kg C m ⁻² yr ⁻¹	m ² m ⁻²	m ² m ⁻²	m ² m ⁻²	kg C m ⁻²
CA	0.68 a	7.47 a	1.98 a	5.49 a	6.68 a
CV	0.64 b	7.15 b	2.11 a	5.04 b	6.30 b
$F_{3,84}$	40.2	57.2	2.96	36.0	11.3
p	<0.001	<0.001	ns	<0.01	<0.001

ns: statistically not significant.

Table 4. Summary of average NPP, LAI and AGB for the Amazon–Cerrado transition zone over the transect domains, considering all P-limitation treatments, regardless of climate and fire presence. One-way ANOVA results are also shown, including F statistics and p values. Values within each column followed by a different letter differ significantly ($p < 0.05$) according to the Tukey–Kramer test ($n = 1240: 31 \text{ pixels} \times 10 \text{ years} \times n_{\text{simulation}}/3$).

Group 2	NPP	LAI _{total}	LAI _{lower}	LAI _{upper}	AGB
	kg C m ⁻² yr ⁻¹	m ² m ⁻²	m ² m ⁻²	m ² m ⁻²	kg C m ⁻²
PC	0.71 a	7.64 a	1.84 b	5.80 a	7.15 a
PR	0.64 b	7.15 b	2.19 a	4.95 b	6.20 b
PG	0.64 b	7.14 b	2.10 a	5.04 b	6.12 b
$F_{2,99}$	62.8	61.0	8.75	53.5	33.6
p	<0.001	<0.001	<0.01	<0.01	<0.001

gion’s greater water availability, which makes the forest naturally fire resistant. Moving into the Cerrado region, on the other hand, a gradient towards seasonally dryer climate increases the intensity and magnitude of fire effects (Fig. 4d). The fire effect on TB over the Amazon domain was 21 to 24 % of the P limitation effect (range for PR and PG cases), while the fire effect on TB over the Cerrado was more than 250 % of the P limitation effects in CV simulations, due to quick growth of grasses after fire occurrence in the latter.

3.1.2 Influence of climate, fire and phosphorus in the transects

Results of the ANOVA and Tukey–Kramer tests indicate that the inclusion of CV, P limitation (PR and PG) and fire in IN-LAND led to significantly different results for average NPP, LAI and AGB in the transition zones. The influences of climate, P and fire are shown separately in Tables 3 to 5 and combined in Table 6.

The inclusion of CV reduces the NPP from 0.68 to 0.64 kg C m⁻² yr⁻¹ (Table 3) and the P-limitation effect reduces NPP from 0.71 to 0.64 kg C m⁻² yr⁻¹ (for both PR and PG; Table 4). The fire effect, on the other hand, has a positive effect on NPP, increasing it from 0.66 kg C m⁻² yr⁻¹ when fire is off to 0.67 kg C m⁻² yr⁻¹ when fire is on. This difference, albeit low, is statistically significant (Table 5).

In addition, both CV and P limitation reduce the LAI_{total} in the canopy (Tables 3 and 4), while the inclusion of fire increases LAI_{lower} more than threefold and decreases LAI_{upper} (Table 5). The effect of including fire on AGB (a 46.7 % decrease, Table 5) is greater in magnitude than the effect of including CV (a 5 % decrease, Table 3) or P limitation (a 14 % decrease, Table 4).

Although CV effects on NPP and AGB for each simulation are not statistically significant, the effects of fire and P limitation (regardless of phosphorus map) are. Fire effects are significant only for structural variables: AGB, LAI_{total}, LAI_{upper} and LAI_{lower}. Simulations showed that LAI_{total} was 1.52 m² m⁻² greater for CV + PG + F as compared to CV + PG, and 1.32 m² m⁻² greater for CV + PR + F as compared to CV + PR (Table 6).

3.1.3 West–east patterns of AGB in the Amazon–Cerrado transition

The model used in this study simulates > 80 % of the observed AGB variability in all treatments along the transition area except in T5 (Table 7). It shows that the model is able to capture AGB variability along the transition area, which is notable when compared to studies that simulate 50 % of the observed AGB variability (Senna et al., 2009; Castanho et al., 2013).

Table 5. Summary of average NPP, LAI and AGB for the Amazon–Cerrado transition zone over the transect domains, considering presence or absence of fire. One-way ANOVA results are also shown, including F statistics and p values. Values within each column followed by a different letter differ significantly ($p < 0.05$) according to the Tukey–Kramer test ($n = 1860$: 31 pixels \times 10 years $\times n_{\text{simulation}}/2$).

Group 3	NPP		LAI _{total}		LAI _{lower}		LAI _{upper}		AGB	
	kg C m ⁻² yr ⁻¹		m ² m ⁻²		m ² m ⁻²		m ² m ⁻²		kg C m ⁻²	
Fire OFF	0.66	a	6.72	b	0.88	b	5.84	a	8.47	b
Fire ON	0.67	b	7.90	a	3.21	a	4.69	b	4.51	a
$F_{3,84}$	8.28		937		1459		249		1719	
p	<0.005		<0.001		<0.01		<0.01		<0.001	

Table 6. Summary of average NPP, LAI and AGB for the Amazon–Cerrado transition zone over the transect domains, considering all factor combinations. One-way ANOVA results are also shown, including F statistics and p values. Values within each column followed by a different letter differ significantly ($p < 0.05$) according to the Tukey–Kramer test ($n = 310$: 31 pixels \times 10 years).

	NPP		LAI _{total}		LAI _{lower}		LAI _{upper}		AGB	
	kg C m ⁻² yr ⁻¹		m ² m ⁻²		m ² m ⁻²		m ² m ⁻²		kg C m ⁻²	
CV + PC	0.69	bcd	6.96	d	0.84	e	6.48	a	9.01	ab
CV + PG	0.61	f	6.24	f	0.85	e	5.60	bc	7.91	c
CV + PR	0.62	f	6.33	f	0.85	e	5.74	bc	8.04	c
CV + PC + F	0.69	abc	7.92	b	2.91	cd	4.61	ef	4.89	de
CV + PG + F	0.63	ef	7.76	b	3.73	a	5.81	bc	3.91	f
CV + PR + F	0.63	ef	7.65	bc	3.47	ab	4.69	ef	4.02	f
CA + PC	0.72	ab	7.39	c	0.91	e	6.12	ab	9.31	a
CA + PG	0.64	def	6.64	e	0.91	e	5.40	cd	8.22	c
CA + PR	0.65	cdef	6.72	de	0.91	e	5.49	cd	8.31	bc
CA + PC + F	0.74	a	8.29	a	2.69	d	5.02	de	5.40	d
CA + PG + F	0.67	cde	7.90	b	3.29	abc	4.04	g	4.45	ef
CA + PR + F	0.67	cde	7.88	b	3.19	bc	4.18	fg	4.42	ef
F	16.2		115		140		38.1		172	
p	<0.001		<0.001		<0.01		<0.01		<0.001	

It is not possible to identify a treatment that best represents AGB for all transects (Table 7). A combined analysis of Table 7 and Fig. 5 indicates a general agreement that observed AGB decreases from west to east in T1 through T4, and this is well captured by several configurations of the model, with specific differences among them. Overall, CA and PC configurations, being the least disturbed treatments, yield higher AGB, while the introduction of CV, PG and F reduce the AGB. However, the simulated results may be above or below the observed ones, which suggests that additional local factors are not included in the model.

The curves of AGB (Fig. 5) show the impact of CV, PG and F along the west-east transition. PG has a high influence on the transition, decreasing the AGB especially in the western part of the transects, where Amazonian vegetation is predominant. This feature is particularly notable in T3 and T4, where PG decreases the AGB by 2 kg C m⁻² in the western pixels of these transects (Fig. 5). In T1, T2 and T5, AGB decline is also higher with P limitation when compared to the curves limited only by CV. However, in T1, model simulations tend to underestimate the highest and the lowest AGB extremes,

and the absolute values were always underestimated, despite the better correlation with the inclusion of the fire component (Table 7).

In T2, T3 and T4, however, fire changes the simulated AGB, making it closer to the observed AGB in the eastern pixels of the Cerrado domain (Fig. 5). In T5, these relationships are similar, with climate having a smaller influence than P on AGB; fire appears mainly to reduce AGB.

3.2 Simulated vegetation composition

Most of the pixels in CA show very robust simulations, with more than 90 % of the same vegetation cover in the last 10 years of simulation (Fig. 6e, m, u, g, o, and w). A larger number of pixels with transitional vegetation were simulated in CV (Fig. 6f, n, v and h, p, x). An even higher variability in CV compared to CA simulations was observed when we added the effects of P limitation and fire (Fig. 6h, p, x).

The vegetation composition in all P-limitation scenarios for CA simulations resulted in robust simulations for nearly all pixels, except for the northern Cerrado domain

Table 7. Correlation coefficients between AGB simulated by INLAND and field estimates ($n = 310$: 31 pixels \times 10 years).

	T1	T2	T3	T4	T5	All transects
CA + PC	0.843	0.928	0.886	0.937	0.337	0.786
CV + PC	0.838	0.884	0.890	0.939	0.355	0.781
CA + PR	0.793	0.848	0.830	0.911	0.399	0.756
CV + PR	0.795	0.793	0.832	0.907	0.527	0.771
CA + PG	0.814	0.951	0.838	0.889	0.388	0.776
CV + PG	0.825	0.922	0.840	0.879	0.496	0.792
CA + PC + F	0.988	0.987	0.977	0.892	0.133	0.795
CV + PC + F	0.976	0.947	0.933	0.908	0.187	0.790
CA + PR + F	0.842	0.805	0.981	0.808	0.561	0.799
CV + PR + F	0.925	0.804	0.927	0.808	0.319	0.757
CA + PG + F	0.844	0.961	0.980	0.830	0.430	0.809
CV + PG + F	0.845	0.932	0.931	0.881	0.177	0.753
CA average	0.854	0.913	0.915	0.878	0.375	0.787
CV average	0.867	0.880	0.892	0.887	0.344	0.774

(Fig. 6e, m, u). The CA + PC and CA + PR simulations had the same vegetation composition, while CA + PG replaced the Tropical Deciduous Forest with Tropical Evergreen Forest in the central Cerrado region, around 8° S, 46° W (Fig. 6a, i, q). This behavior might be related to the higher P_{total} values in PG than PR and PC for the Cerrado region (Fig. S1 in the Supplement). The Cerrado was better represented in CV + PC, CV + PR and CV + PG than in the same CA combinations (Fig. 6). The occurrence of forested areas in the central Cerrado decreased in CV treatments, where it was replaced by the Savanna or Grassland vegetation class.

When the effect of fire was added to CA simulations, the model simulated an increase in the uncertainty of the vegetation cover classification in the Cerrado region. Fire in the CA + PC + F simulation reduced the Tropical Deciduous Forest in the central Cerrado biome, and the vegetation was replaced by Tropical Evergreen Forest in about 5 pixels that have clay soils with large water retention capacity (Fig. 6a and c). In this situation, where there is little water stress, both evergreen and drought-deciduous PFTs have a very high LAI. Fire, although active, is probably too small to be relevant in a non-stressed ecosystem. In CV simulations, however, fire results in the replacement of the Tropical Deciduous and Evergreen Forest by Savanna and Grassland in the entire central Cerrado region (Fig. 6d, l, t). These results show the limitations of CA and the importance of considering interannual climate variability in simulations to improve the accuracy of simulated vegetation as compared to observed.

For all treatments, transitional forest areas in the northern and southwestern Cerrado biome are not adequately represented. With > 90 % of concordance, INLAND assigns Tropical Evergreen Forest rather than Tropical Deciduous Forest in some pixels in the north of the transition area, and Tropical Evergreen Forest rather than Savanna in the southwest, indicating difficulty in simulating transitional vegetation in these regions.

4 Discussion

The inclusion of CV, PR, PG and fire in INLAND revealed significant influences on the simulated vegetation structure and dynamics of the Amazon–Cerrado border (Fig. 4 and Table 6), suggesting that these factors play a key role in determining vegetation structure of the forest–savanna border and can improve the simulated representation of the current contact zone between these biomes. This is broadly consistent with the literature that investigated causes of savanna existence in the real world (Hoffmann et al., 2012; Dantas et al., 2013; Lehmann et al., 2014). In this study, the spatial analysis and the Tukey–Kramer test (TK) show a difference in magnitude among these factors in vegetation, with fire occurrence and P limitation being stronger than interannual climate variability along the transects (Fig. 4).

The spatial analysis showed that CV reduces TB especially in eastern Amazonia (Fig. 4a). Climate of this region is intensely affected by ENSO, which can reduce precipitation by 50 %, placing the vegetation under intense water stress (Botta and Foley, 2002; Foley et al., 2002; Marengo et al., 2004; Andreoli et al., 2012; Hilker et al., 2014). This reduction in rainfall in dry years induces direct changes in carbon flux (NPP) and stocks in leaves and wood, leading to changes in vegetation structure. In addition to interannual changes in rainfall, interannual variability in other climate variables in CV also affects AGB (namely average, maximum and minimum temperatures, wind speed, and specific humidity), and influences photosynthesis in the model, both directly (through Collatz and Farquhar equations) and indirectly (e.g. through evapotranspiration). Our results showed significant differences for most parts of the biomes, except central Amazonia (Fig. 4a), where CV and precipitation seasonality have been noted as secondary effects on vegetation (Restrepo-Coupe et al., 2013), since there is no shortage of water available during the dry season.

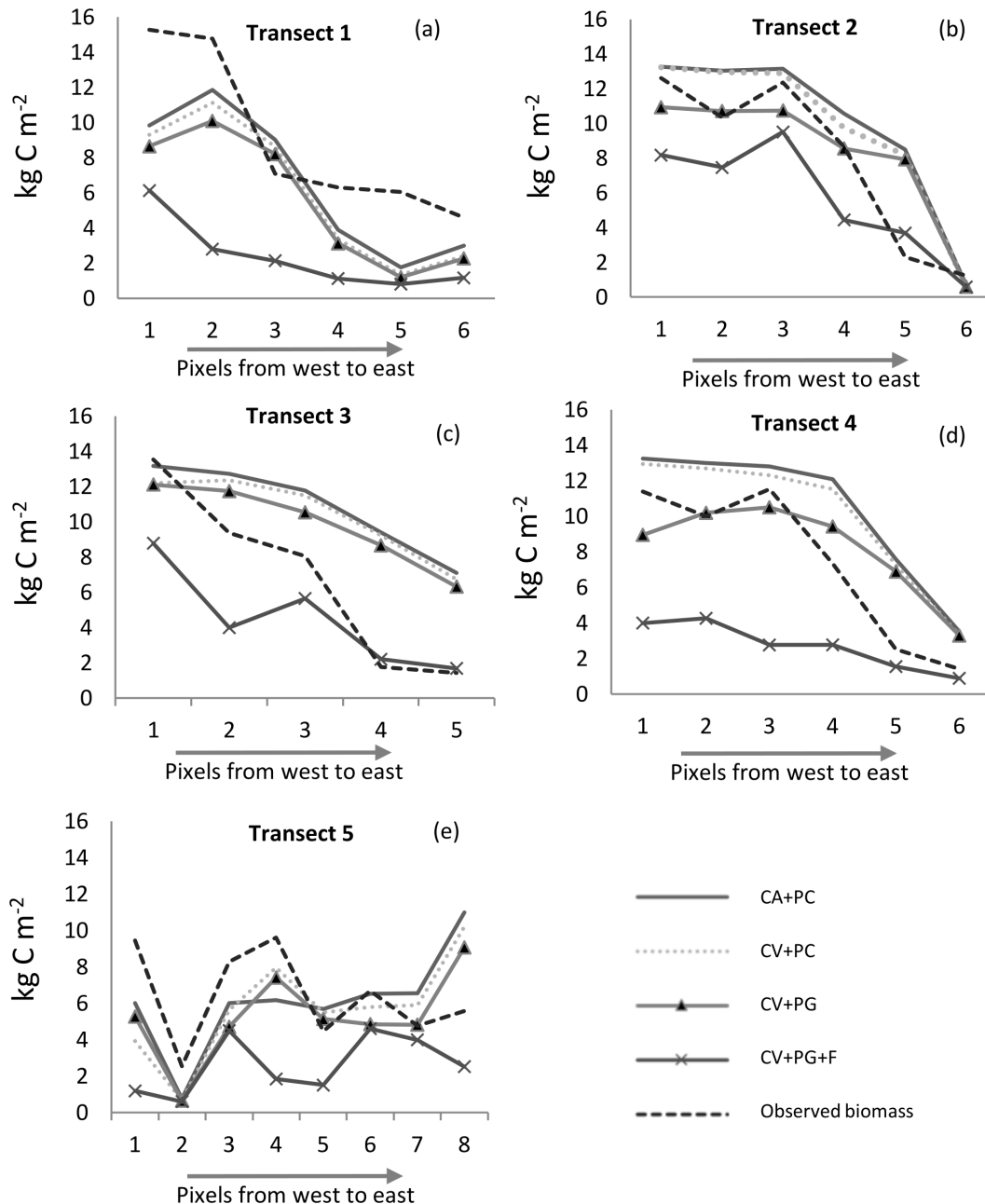


Figure 5. Average longitudinal AGB gradient in the Amazon–Cerrado transition simulated for T1 to T5 (a–e) considering different combinations of factors represented in the simulations: seasonal climate simulation (control) (CA + PC); interannual climate variability simulation (CV + PC); interannual climate variability + global P limitation simulation (CV + PG); and interannual climate variability + P limitation + fire occurrence simulation (CV + PG + F). Observed AGB is also shown for comparison with simulation results.

Across the Cerrado, lower water availability in some years in CV affects tree biomass, despite the fact the vegetation is predominantly grassy–herbaceous. The TB decline is significant for most of the simulated Cerrado domain (Fig. 4a), and average values could represent half the amount of typical tree biomass in this biome, reflecting INLAND’s ability to simulate similar Cerrado conditions and expose the few trees to high water stress.

However, no significant difference in average AGB was found throughout the transects between CV + PC and CA + PC (TK, $p < 0.05$; Table 6). On the other hand, when we analyzed the influence of CV for the same pixels across all simulations (Table 3), the results showed that the decrease in AGB by 0.38 kg C m^{-2} (5.7 %) is statistically significant along the transition, regardless of P limitation and fire occurrence.

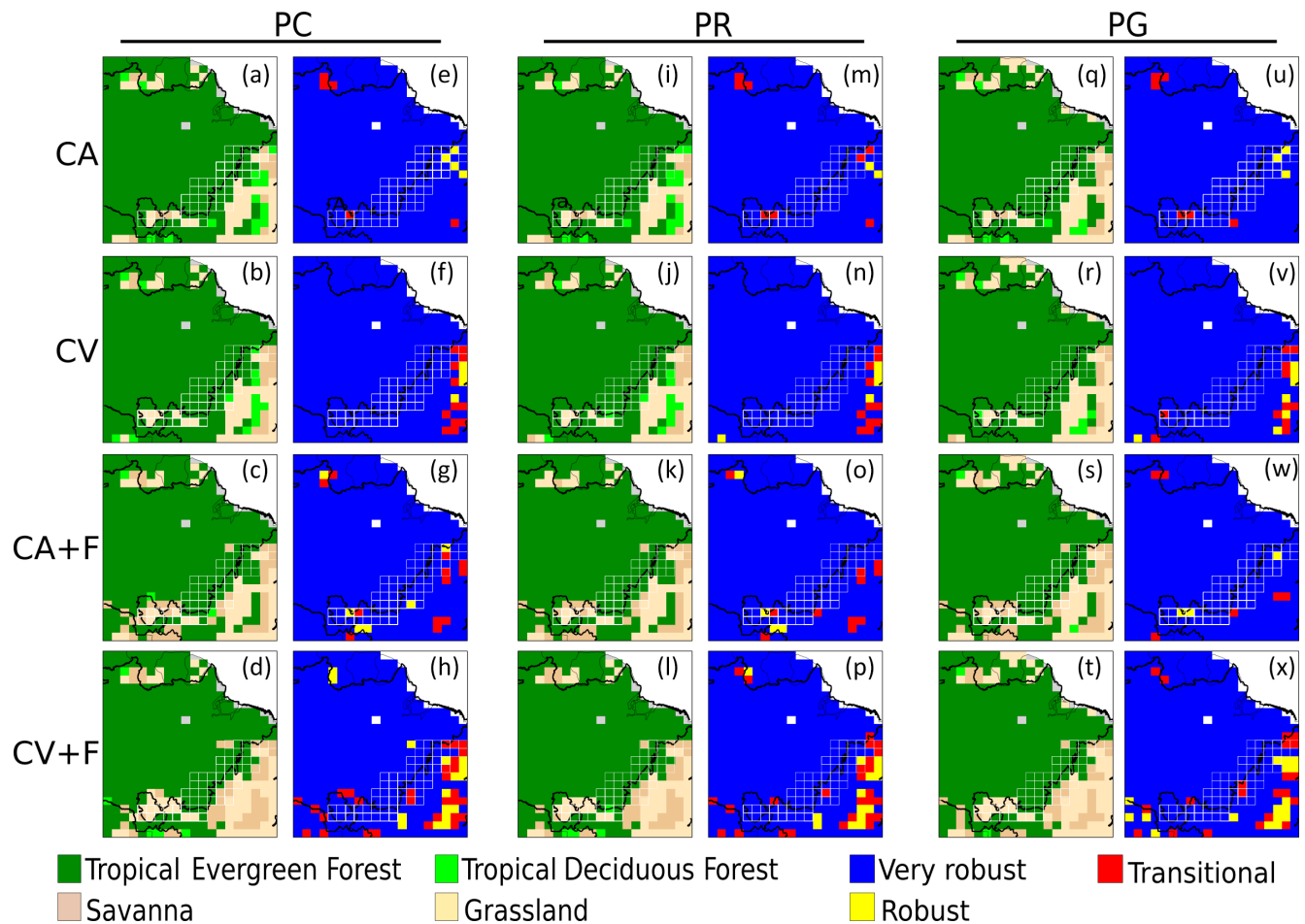


Figure 6. Results for the dominant vegetation cover simulated by INLAND for the different treatments (a–d, i–l, q–t) and a metric of variability in results (e–h, m–p, u–x). Simulations are considered very robust if the dominant vegetation agrees in 9–10 of the last 10 years of simulation, robust if it agrees in 7–8 years, and transitional if it agrees in 6 or fewer years.

The P-limitation effect was statistically significant for PR and PG throughout the Amazon domain, and the main differences between these simulations were the spatial patterns of reduced tree AGB (Fig. 4b–c). We cannot affirm which of these databases is better, since they were derived using different methodologies and observations (Quesada et al., 2010; Yang et al., 2014). However, PG showed a higher TB decrease in central Amazonia, northeastern Pará and northeastern Mato Grosso states, indicating that in these areas the P limitation is higher. This result does not corroborate the northwest–southeast AGB gradient found in the Amazon basin, where studies have shown higher productivity in the west, where soils are more fertile than those found in the southeast (Saatchi et al., 2007; Aragão et al., 2009; Nunes et al., 2012; Lee et al., 2013). On the other hand, PR TB agrees with the northwest–southeast gradient, suggesting less P limitation in the soils of central Amazonia, with declines in TB mainly in the southeastern part of the rainforest (between Pará and northeastern Mato Grosso states; Fig. 4b).

In the Cerrado, P limitation also influenced vegetation (Fig. 4c) and presented statistically significant differences when we compared (CV + PG) minus (CV + PC). In this biome, as well as in the Amazon, tree abundance, richness and diversity have been generally associated with higher soil fertility (Long et al., 2012; Vourtilis et al., 2013), highlighting the importance of P in the composition and maintenance of vegetation, especially in transition areas.

Compared to the Amazon domain, the effects of P limitation are smaller in the Cerrado. However, a few pixels in PR that have P limitation showed a significant decrease in arboreal AGB (Fig. 4b). In PG, we found a reduction of TB for most of the Cerrado domain, except for the southern part of Tocantins state (Fig. 4c). Despite the differences in spatial patterns, there were no statistically significant differences between PR and PG within the transects (Tables 4 and 6).

The spatial differences between PG and PR revealed that PG is lower than PR in western Amazonia and higher in northern Amazonia. Moreover, PG has lower P values in the southern part of the transition compared to PR, while in the

Cerrado domain P values ranged from 120 to 200 mg kg⁻¹ (Fig. S1). Although the PR data set includes all known P data collected in the region, these differences reinforce the need to improve the data on P_{total} for the soils of the Amazon and the Amazon–Cerrado transition domains. Currently, P_{total} data for the Cerrado is scarce, making it unfeasible to establish a proxy similar to Castanho et al. (2013), which was specific for the Amazon.

In INLAND, the inclusion of P limitation, parameterized simply through the linear relationship between V_{max} and P_{total}, showed significant spatial differences in simulated TB and an improvement in simulation accuracy, highlighting the importance of P limitation in modeling studies. For the most part, DGVMs do not consider the complete phosphorus cycle (see exceptions in Goll et al., 2012 and Yang et al., 2014), despite the importance of nutrient cycling for AGB maintenance and tropical vegetation dynamics in dystrophic soils. For example, nutrient cycling in the Amazon–Cerrado transition region is closely related to the hyper-dynamic turnover of AGB (Valadão et al., 2016). Vegetation sustains the constant input of nutrients, including large annual amounts of available P, and in fact some key species might be crucial to the hyper-cycling of nutrients (Oliveira et al., 2017). In addition, weather can affect nutrient fluxes: intense rain can leach nutrients such as nitrogen and strong winds can transport clay particles on which nutrients are adsorbed. However, in this work, nutrient conditions are prescribed and fixed.

Fire occurrence is another important factor that controls AGB dynamics in the Cerrado and in transitional vegetation (Hoffman et al., 2003; Hoffman et al., 2012; Silvério et al., 2013; Couto-Santos et al., 2014; Balch et al., 2015). This study clearly corroborates these findings, showing statistically significant influences of fire when compared to control simulations (Fig. 4d and Table 5). In the transition region, the fire effect may reduce average AGB by 50 % (Table 5), which under climate change or deforestation conditions may lead to an even stronger change in the vegetation structure and dynamics. As stated in Sect. 2.2, fire in INLAND acts on upper- and lower-canopy LAI according to fire occurrence, triggering competition. The changes in canopy structure after fire occurrence are exclusively due to the canopy opening and consequently allowing more penetration of photosynthetic radiation into the lower canopy. This competition induces a significant increase in the lower canopy, resulting in increased LAI_{lower} (Table 5).

The model does not include fire characteristics such as velocity, intensity and duration of burning (Hoffman et al., 2003; Rezende et al., 2005; Elias et al., 2013; Reis et al., 2015) or the representation of some tree morphological adaptations, such as bark thickness, that confer fire resilience to Cerrado species. Thus, trees and grasses throughout the Amazon–Cerrado border area are equally affected by occurrence of fire within a grid cell. However, despite these limitations in the representation of fire characteristics and morphological attributes of fire resistance, our results show that

simulated biomass is closer to observed biomass in Cerrado areas when the fire module is activated (Fig. 5). An improvement in the distribution of biomes along the simulated transition area is also observed (Fig. 6d, l, t), highlighting fire as an essential factor in representing the Amazon–Cerrado border.

This study shows better correlation between simulated and observed AGB when compared to previous modeling studies, regardless of treatment. The correlation coefficients are generally above 0.80 for the transects except for T5, for which the correlation coefficient is generally below 0.5 (Table 7). Senna et al. (2009) found a maximum correlation coefficient between simulated and observed AGB of 0.20, while Castanho et al. (2013) showed a correlation coefficient of 0.80 for the Amazon domain. From Fig. 5, it is clear that CV, F and P limitation in the transition zone reduce AGB, causing the simulated data to approach the observed data. However, the inclusion of these effects is still insufficient to represent the correct distribution of vegetation types throughout the Amazon–Cerrado border region (Fig. 6t). In our interpretation, this means that other important factors still need to be represented, especially in T5, where soils are rocky and shallow. Better spatial representation of soil physical properties (including shallow, rocky soils) are probably needed. Additionally, spatially varying physiological parameterizations of the vegetation (such as carbon allocation, deciduousness of vegetation and residence time) and improved representation of fire and vegetation fire resistance are probably needed to improve the accuracy of simulations, in particular in the northern and southern extremes of the border region (T1 and T5).

For all transects, the AGB curves have similar patterns (Fig. 5); smaller differences are observed between the CA + PC and CV + PG curves, while larger differences are observed when fire is present. The effect of P limitation is intermediate in magnitude, but it reduces AGB more than including interannual climate variability does. In the east, it is observed that there is little or no difference among AGB simulated with CA + PC, CV + PC and CV + PG, revealing that interannual climate variability and P have a smaller influence on the AGB there. In the east of T2, T3 and T4, fire is the factor that brings the simulated results closest to the observed data (Fig. 5); this differs from the results for the western grid points, where CV + PG appears to be a better proxy for observed data.

These results are interesting because they reflect the different mechanisms that regulate the structure of these ecosystems and probably the vegetation structure and distribution in different locations. For example, P limitation seems to be the factor that improves simulated AGB in regions where the predominant vegetation type is tropical rainforest. Fire, on the other hand, improves the representation of AGB in grid points where Cerrado vegetation occurs. Moreover, important factors such as partitioning productivity into leaves, roots and wood carbon pools are assumed to be fixed in space and time within a given PFT, neglecting the natural

capacity of transitional forests to adapt and to adjust their metabolisms to local environmental conditions (Senna et al., 2009). In years of severe drought or under frequent fire occurrence, transitional forests can (1) prioritize the stock of carbon in fine roots instead of the basal or leaf increment in order to maximize access to water, (2) undergo hydraulic redistribution of soil moisture to maintain greenness and photosynthesis rates, or (3) increase the capacity to resprout after fire occurrence (Hoffman et al., 2003; Brando et al., 2008). Brando et al. (2008) found changes in carbon allocation after an artificial drought in eastern Amazonia, with wood production reduced 13–60 % and an associated increase in root production. Although in INLAND low soil moisture can reduce photosynthetic rates, carbon allocation rates are fixed (Fig. 5a).

T2, T3 and T4, located in the central part of the Amazon–Cerrado transition, showed the highest average correlations between observed and simulated data (Table 7). For these transects, INLAND seems to be able to capture the high variability in the AGB gradient.

At T5, located at the south of the transition area, average correlations were low for all treatments, indicating that INLAND has difficulty representing the AGB gradient in that region (Table 7). However, it captures the lower AGB as compared to the northern areas. In this region, the vegetation is characterized by a wide diversity of characteristics, which vary along with other important factors, such as lithology, soil depth, topography and soil fertility. The observed data also showed high AGB variability, indicating that there are changes in the vegetation structure for this area featuring medium-sized and small vegetation types on different soil types. In INLAND, however, features such as lithology and water-table depth are not considered due to the complexity of representing them on a large scale; this limits the model's ability to represent heterogeneous environments throughout the transitional region.

Patterns of vegetation distribution along the Amazon–Cerrado border are influenced not only by interannual climate variability, P limitation, and fire but also by ecophysiological parameters. Additional field experiments are needed to understand relationships among currently fixed parameters (such as carbon allocation, residence time and deciduousness), environmental conditions and soil properties.

5 Conclusions

This is the first study that uses modeling to assess the influence of interannual climate variability, fire occurrence and P limitation to represent the Amazon–Cerrado border. This study shows that, although the model forced by a climatological database is able to simulate basic characteristics of the Amazon–Cerrado transition, the addition of factors such as interannual climate variability, P limitation and fire improves simulation of vegetation types. These effects are not homogeneous throughout the region, which makes the adequate sim-

ulation of biomass challenging in some places. Based on the *F* statistic reported in Tables 3–5, fire is the main factor determining changes in vegetation structure (LAI, AGB) along the transition. P limitation is second in magnitude, stronger than the effect of interannual climate variability.

Overall, although INLAND typically simulates more than 80 % of the variability of biomass in the transition zone, in many places the biomass is clearly not well simulated. Situations for markedly wet or dry climate conditions were well simulated, but the simulations are generally poor for transitional areas where the environment selected physiognomies that have an intermediate behavior, as is the case for transitional forests in northern Tocantins and Mato Grosso.

There is evidence that the inclusion of spatially explicit parameters such as woody biomass residence time, maximum carboxylation capacity (V_{\max}), and NPP allocation to wood may improve Amazon rainforest AGB simulation by DGVMs (Castanho et al., 2013). However, in the transitional area, the lack of measured field parameters limits inclusion of the variability in these biophysical parameters in DGVMs. Additional field work and compilation of existing data are necessary to obtain physiological and structural parameters throughout the Amazon–Cerrado border area to establish numerical relationships between soil, climate and vegetation. With the help of these data, dynamic vegetation models will be able to improve simulation of current patterns and future changes in vegetation considering climate change scenarios. In addition, it is necessary to include not only spatial variability but also temporal variability in physiological parameters of vegetation, allowing more realistic simulation of soil–climate–vegetation relationships. Finally, our results reinforce the need for DGVMs to incorporate nutrient limitation and fire occurrence for simulating the Amazon–Cerrado border position.

Data availability. Data presented in this article are available from the first author upon request (emily.ane@gmail.com) and in Table S2 in the Supplement.

The Supplement related to this article is available online at <https://doi.org/10.5194/bg-15-919-2018-supplement>.

Competing interests. The authors declare that they have no conflict of interest.

Acknowledgements. We gratefully thank the Brazilian agencies FAPEMIG and CAPES for their financial support. Atul K. Jain is funded by the US National Science Foundation (NSF-AGS-12-43071).

Edited by: Anja Rammig

Reviewed by: three anonymous referees

References

- Andreoli, R. V., Ferreira de Souza, R. A., Kayano, M. T., and Candido, L. A.: Seasonal anomalous rainfall in the central and eastern Amazon and associated anomalous oceanic and atmospheric patterns, *Int. J. Climatol.*, 32, 1193–1205, <https://doi.org/10.1002/joc.2345>, 2012.
- Aragão, L. E. O. C., Malhi, Y., Metcalfe, D. B., Silva-Espejo, J. E., Jiménez, E., Navarrete, D., Almeida, S., Costa, A. C. L., Salinas, N., Phillips, O. L., Anderson, L. O., Alvarez, E., Baker, T. R., Goncalvez, P. H., Huamán-Ovalle, J., Mamani-Solórzano, M., Meir, P., Monteagudo, A., Patiño, S., Peñuela, M. C., Prieto, A., Quesada, C. A., Rozas-Dávila, A., Rudas, A., Silva Jr., J. A., and Vásquez, R.: Above- and below-ground net primary productivity across ten Amazonian forests on contrasting soils, *Biogeosciences*, 6, 2759–2778, <https://doi.org/10.5194/bg-6-2759-2009>, 2009.
- Arora, V. K. and Boer, G. J.: Fire as an interactive component of dynamic vegetation models, *J. Geophys. Res.*, 110, G02008, <https://doi.org/10.1029/2005JG000042>, 2005.
- Balch, J. K., Brando, P. M., Nepstad, D. C., Coe, M. T., Silvério, D., Massad, T. J., Davidson, E. A., Lefebvre, P., Oliveira-Santos, C., Rocha, W., Cury, R. T. S., Parsons, A., and Carvalho, K. S.: The Susceptibility of Southeastern Amazon Forests to Fire: Insights from a Large-Scale Burn Experiment, *Bioscience*, 65, 893–905, <https://doi.org/10.1093/biosci/biv106>, 2015.
- Beguería, S., Vicente-Serrano, S. M., Tomás-Burguera, M., and Maneta, M.: Bias in the variance of gridded data sets leads to misleading conclusions about changes in climate variability. *Int. J. Climatol.*, 36, 3413–3422, <https://doi.org/10.1002/joc.4561>, 2016.
- Betts, R. A., Cox, P. M., Collins, M., Harris, P. P., Huntingford, C., and Jones, C. D.: The role of ecosystem-atmosphere interactions in simulated Amazonian precipitation decrease and forest dieback under global climate warming, *Theor. Appl. Climatol.*, 78, 157–175, <https://doi.org/10.1007/s00704-004-0050-y>, 2004.
- Bonan, G. B.: Forests and climate change: forcings, feedbacks, and the climate benefits of forests, *Science*, 320, 1444–1449, <https://doi.org/10.1126/science.1155121>, 2008.
- Bond, W. J., Woodward, F. I., and Midgley, G. F.: The global distribution of ecosystems in a world without fire, *New Phytol.*, 165, 525–538, <https://doi.org/10.1111/j.1469-8137.2004.01252.x>, 2005.
- Botta, A. and Foley, J. A.: Effects of climate variability and disturbances on the Amazonian terrestrial ecosystems dynamics, *Global Biogeochem. Cy.*, 16, 1070, <https://doi.org/10.1029/2000GB001338>, 2002.
- Brando, P. M., Nepstad, D. C., Davidson, E. A., Trumbore, S. E., Ray, D., and Camargo, P.: Drought effects on litterfall, wood production and belowground carbon cycling in an Amazon forest: results of a throughfall reduction experiment, *Philos. T. Roy. Soc. B*, 363, 1839–1848, <https://doi.org/10.1098/rstb.2007.0031>, 2008.
- Castanho, A. D. A., Coe, M. T., Costa, M. H., Malhi, Y., Galbraith, D., and Quesada, C. A.: Improving simulated Amazon forest biomass and productivity by including spatial variation in biophysical parameters, *Biogeosciences*, 10, 2255–2272, <https://doi.org/10.5194/bg-10-2255-2013>, 2013.
- Couto-Santos, F. R., Luizão, F. J., and Carneiro Filho, A.: The influence of the conservation status and changes in the rainfall regime on forest-savanna mosaic dynamics in Northern Brazilian Amazonia, *Acta Amazon*, 44, 197–206, 2014.
- Cox, P. M., Betts, R. A., Jones, C. D., Spall, S. A., and Totterdell, I. J.: Acceleration of global warming due to carbon-cycle feedbacks in a coupled climate model, *Nature*, 408, 184–187, <https://doi.org/10.1038/35041539>, 2000.
- Cox, P. M., Betts, R. A., Collins, M., Harris, P. P., Huntingford, C., and Jones, C. D.: Amazonian forest dieback under climate-carbon cycle projections for the 21st century, *Theor. Appl. Climatol.*, 78, 137–156, <https://doi.org/10.1007/s00704-004-0049-4>, 2004.
- Dajoz, R.: *Princípios de ecologia*, 7^o edição, Artmed, Porto Alegre, RS, Brazil, 519 pp., 2005.
- Dantas, V. L., Batalha, M. A., and Pausas, J. G.: Fire drives functional thresholds on the savanna-forest transition, *Ecology*, 94, 2454–2463, <https://doi.org/10.1890/12-1629.1>, 2013.
- da Rocha, H. R., Goulden, M. L., Miller, S. D., Menton, M. C., Pinto, L. D. V. O., De Freitas, H. C., and Figueira, A. M. E. S.: Seasonality of water and heat fluxes over a tropical forest in eastern Amazonia, *Ecol. Appl.*, 14, 22–32, <https://doi.org/10.1890/02-6001>, 2004.
- Davidson, E. A., Carvalho, C. J. R., Vieira, I. C. G., Figueiredo, R. D. O., Moutinho, P., Ishida, F. Y., Santos, M. T. P., Guerrero, J. B., Kalif, K., and Sabá, R. T.: Nitrogen and Phosphorus Limitation of Biomass Growth in a Tropical Secondary Forest, *Ecol. Appl.*, 14, 150–163, <https://doi.org/10.1890/01-6006>, 2004.
- Elias, F., Marimon, B. S., Matias, S. R. A., Forsthofer, M., Morandi, P. S. and Marimon-Junior, B. H.: Dinâmica da distribuição espacial de populações arbóreas, ao longo de uma década, em cerrado na transição Cerrado-Amazônia, *Mato Grosso, Biota Amaz.*, 3, 1–14, 2013.
- Favier, C., Chave, J., Fabing, A., Schwartz, D., and Dubois, M. A.: Modelling forest-savanna mosaic dynamics in man-influenced environments: Effects of fire, climate and soil heterogeneity, *Ecol. Model.*, 171, 85–102, <https://doi.org/10.1016/j.ecolmodel.2003.07.003>, 2004.
- Foley, J. A., Prentice, I. C., Ramankutty, N., Levis, S., Pollard, D., Sitch, S., and Haxeltine, A.: An integrated biosphere model of land surface processes, terrestrial carbon balance, and vegetation dynamics, *Global Biogeochem. Cy.*, 10, 603–628, <https://doi.org/10.1029/96GB02692>, 1996.
- Foley, J. A., Botta, A., Coe, M. T., and Costa, M. H.: El Niño–Southern oscillation and the climate, ecosystems and rivers of Amazonia, *Global Biogeochem. Cy.*, 16, 79–1–79–20, <https://doi.org/10.1029/2002GB001872>, 2002.
- Goedert, W.: *Solos do Cerrado: Tecnologias e Estratégias de Manejo*, Empresa Brasileira de Pesquisa Agropecuária (EMBRAPA), Brasília, DF, Brasil, 422 pp., 1986.
- Goll, D. S., Brovkin, V., Parida, B. R., Reick, C. H., Kattge, J., Reich, P. B., van Bodegom, P. M., and Niinemets, Ü.: Nutrient limitation reduces land carbon uptake in simulations with a model of combined carbon, nitrogen and phosphorus cycling, *Biogeosciences*, 9, 3547–3569, <https://doi.org/10.5194/bg-9-3547-2012>, 2012.
- Hansen, M. C. and Reed, B.: A comparison of the IGBP DISCover and University of Maryland 1 km global land cover products, *Int. J. Remote Sens.*, 21, 1365–1373, <https://doi.org/10.1080/014311600210218>, 2000.

- Harris, I., Jones, P. D., Osborn, T. J., and Lister, D. H.: Updated high-resolution grids of monthly climatic observations – the CRU TS3.10 Dataset, *Int. J. Climatol.*, 34, 623–642, <https://doi.org/10.1002/joc.3711>, 2014.
- Hilker, T., Lyapustin, A. I., Tucker, C. J., Hall, F. G., Myrneni, R. B., Wang, Y., Bi, J., Mendes de Moura, Y., and Sellers, P. J.: Vegetation dynamics and rainfall sensitivity of the Amazon., *P. Natl. Acad. Sci. USA*, 111, 16041–16046, <https://doi.org/10.1073/pnas.1404870111>, 2014.
- Hirota, M., Nobre, C., Oyama, M. D., and Bustamante, M. M. C.: The climatic sensitivity of the forest, savanna and forest-savanna transition in tropical South America, *New Phytol.*, 187, 707–719, <https://doi.org/10.1111/j.1469-8137.2010.03352.x>, 2010.
- Hoffmann, W. A., Orthen, B., and P. K. V. Nascimento.: Comparative fire ecology of tropical savanna and forest trees, *Funct. Ecol.*, 17, 720–726, 2003.
- Hoffmann, W. A., Geiger, E. L., Gotsch, S. G., Rossatto, D. R., Silva, L. C. R., Lau, O. L., Haridasan, M., and Franco, A. C.: Ecological thresholds at the savanna-forest boundary: How plant traits, resources and fire govern the distribution of tropical biomes, *Ecol. Lett.*, 15, 759–768, <https://doi.org/10.1111/j.1461-0248.2012.01789.x>, 2012.
- House, J. I., Archer, S., Breshears, D. D., and Scholes, R. J.: Conundrums in mixed woody-herbaceous plant systems, *J. Biogeogr.*, 30, 1763–1777, <https://doi.org/10.1046/j.1365-2699.2003.00873.x>, 2003.
- IBGE: Manual Técnico da Vegetação Brasileira (Manuais Técnicos em Geociências n. 1), Fundação Instituto Brasileiro de Geografia e Estatística (IBGE), Rio de Janeiro, RJ, Brasil, 92 pp., 1992.
- IBGE: Mapa da Vegetação do Brasil, Fundação Instituto Brasileiro de Geografia e Estatística (IBGE), Rio de Janeiro, RJ, Brazil, Map, 2004.
- Klink, C. A. and Machado, R. B.: Conservation of the Brazilian Cerrado, *Conserv. Biol.*, 19, 707–713, <https://doi.org/10.1111/j.1523-1739.2005.00702.x>, 2005.
- Kucharik, C. J., Foley, J. A., Delire, C., Fisher, V. A., Coe, M. T., Lenters, J. D., Young-Molling, C., Ramankutty, N., Norman, J. M., and Gower, S. T.: Testing the performance of a Dynamic Global Ecosystem Model: Water balance, carbon balance, and vegetation structure, *Global Biogeochem. Cy.*, 14, 795–825, <https://doi.org/10.1029/1999GB001138>, 2000.
- Lee, J. E., Frankenberg, C., van der Tol, C., Berry, J. A., Guanter, L., Boyce, C. K., Fisher, J. B., Morrow, E., Worden, J. R., Asefi, S., Badgley, G., and Saatchi, S.: Forest productivity and water stress in Amazonia: observations from GOSAT chlorophyll fluorescence, *Proc. R. Soc. Ser. B-Biol.*, 280, 20130171–20131761, <https://doi.org/10.1098/rspb.2013.0171>, 2013.
- Lehmann, C. E. R., Archibald, S. A., Hoffmann, W. A., and Bond, W. J.: Deciphering the distribution of the savanna biome, *New Phytol.*, 191, 197–209, <https://doi.org/10.1111/j.1469-8137.2011.03689.x>, 2011.
- Lehmann, C. E. R., Anderson, T. M., Sankaran, M., Higgins, S. I., Archibald, S., Hoffmann, W. A., Hanan, N. P., Williams, R. J., Fensham, R. J., Felfili, J., Hutley, L. B., Ratnam, J., Jose, J. S., Montes, R., Franklin, D., Russell-Smith, J., Ryan, C. M., Durigan, G., Hiernaux, P., Haidar, R., Bowman, D. M. J. S., and Bond, W. J.: Savanna Vegetation–Fire–Climate Relationships Differ Among Continents, *Science*, 343, 548–553, <https://doi.org/10.1126/science.1247355>, 2014.
- Long, W., Yang, X., and Donghai, L.: Patterns of species diversity and soil nutrients along a chronosequence of vegetation recovery in Hainan Island, South China, *Ecol. Res.*, 27, 561–568, 2012.
- Malhi, Y., Aragão, L. E. O. C., Metcalfe, D. B., Paiva, R., Quezada, C. A., Almeida, S., Anderson, L., Brando, P., Chambers, J. Q., da Costa, A. C. L., Hutryra, L. R., Oliveira, P., Patiño, S., Pyle, E. H., Robertson, A. L., and Teixeira, L. M.: Comprehensive assessment of carbon productivity, allocation and storage in three Amazonian forests, *Glob. Chang. Biol.*, 15, 1255–1274, <https://doi.org/10.1111/j.1365-2486.2008.01780.x>, 2009.
- Marengo, J. A.: Interdecadal variability and trends of rainfall across the Amazon basin, *Theor. Appl. Climatol.*, 78, 79–96, <https://doi.org/10.1007/s00704-004-0045-8>, 2004.
- Marimon, B. S., Lima, E. S., Duarte, T. G., Chieregatto, L. C., and Ratter, J. A.: Observations on the vegetation of north-eastern Mato Grosso, Brazil. IV. An analysis of the Cerrado–Amazonian Forest ecotone, *Edinburgh Journal of Botany*, 63, 323–341, <https://doi.org/10.1017/S0960428606000576>, 2006.
- Marimon, B. S., Marimon-Junior, B. H., Feldpausch, T. R., Oliveira-Santos, C., Mews, H. A., Lopez-Gonzalez, G., Lloyd, J., Franczak, D. D., de Oliveira, E. A., Maracchipes, L., Miguel, A., Lenza, E., and Phillips, O. L.: Disequilibrium and hyperdynamic tree turnover at the forest–cerrado transition zone in southern Amazonia, *Plant Ecol. Divers.*, 7, 281–292, <https://doi.org/10.1080/17550874.2013.818072>, 2014.
- Marimon-Junior, B. H. and Haridasan, M.: Comparação da vegetação arbórea e características edáficas de um cerrado e um cerrado sensu stricto em áreas adjacentes sobre solo distrófico no leste de Mato Grosso, Brasil, *Acta Bot. Bras.*, 19, 913–926, <https://doi.org/10.1590/S0102-33062005000400026>, 2005.
- Mercado, L. M., Patino, S., Domingues, T. F., Fyllas, N. M., Weedon, G. P., Sitch, S., Quesada, C. A., Phillips, O. L., Aragao, L. E. O. C., Malhi, Y., Dolman, A. J., Restrepo-Coupe, N., Saleska, S. R., Baker, T. R., Almeida, S., Higuchi, N., and Lloyd, J.: Variations in Amazon forest productivity correlated with foliar nutrients and modelled rates of photosynthetic carbon supply, *Philos. T. Roy. Soc. B.*, 366, 3316–3329, <https://doi.org/10.1098/rstb.2011.0045>, 2011.
- Morandi, P. S., Marimon-Junior, B. H., Oliveira, E. A., Reis, S. M. A., Valadão, M. B. X., Forsthofer, M., Passos, F. B., and Marimon, B. S.: Vegetation Succession in the Cerrado–Amazonian Forest Transition Zone of Mato Gross State, Brazil, *Edinburgh Journal of Botany*, 73, 83–93, <https://doi.org/10.1017/S096042861500027X>, 2016.
- Moreno, M. I. C., Schiavini, I., and Haridasan, M.: Fatores edáficos influenciando na estrutura de fitofisionomias do cerrado, *Caminhos da Geogr.*, 9, 173–194, 2008.
- Murphy, B. P. and Bowman, D. M. J. S.: What controls the distribution of tropical forest and savanna?, *Ecol. Lett.*, 15, 748–758, <https://doi.org/10.1111/j.1461-0248.2012.01771.x>, 2012.
- Myers, N., Mittermeier, R. A., Mittermeier, C. G., Fonseca G. A. B., and Kent, J.: Biodiversity hotspots for conservation priorities, *Nature*, 403, 853–858, <https://doi.org/10.1038/35002501>, 2000.
- Nardoto, G. B., Bustamante, M. M. C., Pinto, A. S., and Klink, C. A.: Nutrient use efficiency at ecosystem and species level in savanna areas of Central Brazil and impacts of fire, *J. Trop. Ecol.*, 22, 191–201, <https://doi.org/10.1017/S0266467405002865>, 2006.
- Nogueira, E. M., Yanai, A. M., Fonseca, F. O., and Fearnside, P. M.: Carbon stock loss from deforestation through 2013

- in Brazilian Amazonia, *Glob. Change Biol.*, 21, 1271–1292, <https://doi.org/10.1111/gcb.12798>, 2015.
- Nunes, E. L., Costa, M. H., Malhado, A. C. M., Dias, L. C. P., Vieira, S. A., Pinto, L. B., and Ladle, R. J.: Monitoring carbon assimilation in South America's tropical forests: Model specification and application to the Amazonian droughts of 2005 and 2010, *Remote Sens. Environ.*, 117, 449–463, <https://doi.org/10.1016/j.rse.2011.10.022>, 2012.
- Oliveira, B., Marimon-Junior, B. H., Mews, H. A., Valadão, M. B. X., and Marimon, B. S.: Unraveling the ecosystem functions in the Amazonia–Cerrado transition: evidence of hyperdynamic nutrient cycling, *Plant Ecol.*, 218, 225–239, <https://doi.org/10.1007/s11258-016-0681-y>, 2017.
- Oyama, M. D. and Nobre, C. A.: A new climate-vegetation equilibrium state for Tropical South America, *Geophys. Res. Lett.*, 30, 10–13, <https://doi.org/10.1029/2003GL018600>, 2003.
- Parton, W. J., Scurlock, J. M. O., Ojima, D. S., Gilmanov, T. G., Scholes, R. J., Schimel, D. S., Kirchner, T., Menaut, J.-C., Seastedt, T., Garcia Moya, E., Kamnalrut, A., and Kinyamario, J. I.: Observations and modeling of AGB and soil organic matter dynamics for the grassland biome worldwide, *Global Biogeochem. Cy.*, 7, 785–809, <https://doi.org/10.1029/93GB02042>, 1993.
- Pereira, M. P. S., Malhado, A. C. M., and Costa, M. H.: Predicting land cover changes in the Amazon rainforest: An ocean-atmosphere-biosphere problem, *Geophys. Res. Lett.*, 39, 1–7, <https://doi.org/10.1029/2012GL051556>, 2012.
- Pires, G. F. and Costa, M. H.: Deforestation causes different subregional effects on the Amazon bioclimatic equilibrium, *Geophys. Res. Lett.*, 40, 3618–3623, <https://doi.org/10.1002/grl.50570>, 2013.
- Quesada, C. A., Lloyd, J., Schwarz, M., Patiño, S., Baker, T. R., Czimczik, C., Fyllas, N. M., Martinelli, L., Nardoto, G. B., Schmerler, J., Santos, A. J. B., Hodnett, M. G., Herrera, R., Luizão, F. J., Arneith, A., Lloyd, G., Dezzio, N., Hilke, I., Kuhlmann, I., Raessler, M., Brand, W. A., Geilmann, H., Moraes Filho, J. O., Carvalho, F. P., Araujo Filho, R. N., Chaves, J. E., Cruz Junior, O. F., Pimentel, T. P., and Paiva, R.: Variations in chemical and physical properties of Amazon forest soils in relation to their genesis, *Biogeosciences*, 7, 1515–1541, <https://doi.org/10.5194/bg-7-1515-2010>, 2010.
- Quesada, C. A., Phillips, O. L., Schwarz, M., Czimczik, C. I., Baker, T. R., Patiño, S., Fyllas, N. M., Hodnett, M. G., Herrera, R., Almeida, S., Alvarez Dávila, E., Arneith, A., Arroyo, L., Chao, K. J., Dezzio, N., Erwin, T., di Fiore, A., Higuchi, N., Honorio Coronado, E., Jimenez, E. M., Killeen, T., Lezama, A. T., Lloyd, G., López-González, G., Luizão, F. J., Malhi, Y., Monteagudo, A., Neill, D. A., Núñez Vargas, P., Paiva, R., Peacock, J., Peñuela, M. C., Peña Cruz, A., Pitman, N., Priante Filho, N., Prieto, A., Ramírez, H., Rudas, A., Salomão, R., Santos, A. J. B., Schmerler, J., Silva, N., Silveira, M., Vásquez, R., Vieira, I., Terborgh, J., and Lloyd, J.: Basin-wide variations in Amazon forest structure and function are mediated by both soils and climate, *Biogeosciences*, 9, 2203–2246, <https://doi.org/10.5194/bg-9-2203-2012>, 2012.
- Reis, S. M., Marimon, B. S., Marimon-Junior, B.-H., Gomes, L., Morandi, P. S., Freire, E. G., and Lenza, E.: Resilience of savanna forest after clear-cutting in the Cerrado–Amazon transition zone, *Bioscience*, 31, 1519–1529, <https://doi.org/10.14393/BJ-v31n5a2015-26368>, 2015.
- Restrepo-Coupe, N., da Rocha, H. R., Hutryra, L. R., da Araujo, A. C., Borma, L. S., Christoffersen, B., Cabral, O. M. R., de Camargo, P. B., Cardoso, F. L., da Costa, A. C. L., Fitzjarrald, D. R., Goulden, M. L., Kruijt, B., Maia, J. M. F., Malhi, Y. S., Manzi, A. O., Miller, S. D., Nobre, A. D., von Randow, C., Sá, L. D. A., Sakai, R. K., Tota, J., Wofsy, S. C., Zanchi, F. B., and Saleska, S. R.: What drives the seasonality of photosynthesis across the Amazon basin? A cross-site analysis of eddy flux tower measurements from the Brazil flux network, *Agr. Forest Meteorol.*, 182–183, 128–144, <https://doi.org/10.1016/j.agrformet.2013.04.031>, 2013.
- Rezende, A. V., Sanquetta, C. R., and Filho, F. A.: Efeito do desmatamento no estabelecimento de espécies lenhosas em um cerrado *Sensu stricto*, *Floresta*, 35, 69–88, 2005.
- Ribeiro, J. F. and Walter, B. M. T.: As Principais Fitofisionomias do bioma Cerrado, in: *Cerrado: ecologia e flora*, Embrapa Cerrados. – Brasília, DF : Embrapa Informação Tecnológica 153–212, 2008.
- Roy, S. B. and Avissar, R.: Impact of land use/land cover change on regional hydrometeorology in Amazonia, *J. Geophys. Res.*, 107, 1–12, <https://doi.org/10.1029/2000JD000266>, 2002.
- Saatchi, S., Houghton, R. A., Dos Santos Alvalá, R. C., Soares, J. V., and Yu, Y.: Distribution of aboveground live AGB in the Amazon basin, *Glob. Change Biol.*, 13, 816–837, <https://doi.org/10.1111/j.1365-2486.2007.01323.x>, 2007.
- Salazar, L. F., Nobre, C. A., and Oyama, M. D.: Climate change consequences on the biome distribution in tropical South America, *Geophys. Res. Lett.*, 34, 2–7, <https://doi.org/10.1029/2007GL029695>, 2007.
- Senna, M. C. A., Costa, M. H., Pinto, L. I. C., Imbuzeiro, H. M. A., Diniz, L. M. F., and Pires, G. F.: Challenges to reproduce vegetation structure and dynamics in Amazonia using a coupled climate-biosphere model, *Earth Interact.*, 13, 1–28, <https://doi.org/10.1175/2009EI281.1>, 2009.
- Shukla, J., Nobre, C., and Sellers, P.: Amazon deforestation and climate change, *Science*, 247, 1322–1325, <https://doi.org/10.1126/science.247.4948.1322>, 1990.
- Silvério, D. V., Brando, P. M., Balch, J. K., Putz, F. E., Nepstad, D. C., and Oliveira-Santos, C., and Bustamante, M. M. C.: Testing the Amazon savannization hypothesis: fire effects on invasion of a neotropical forest by native cerrado and exotic pasture grasses, *Philos. T. Roy. Soc. B.*, 368, 20120427 <https://doi.org/10.1098/rstb.2012.0427>, 2013.
- Smith, B., Wårlind, D., Arneith, A., Hickler, T., Leadley, P., Siltberg, J., and Zaehle, S.: Implications of incorporating N cycling and N limitations on primary production in an individual-based dynamic vegetation model, *Biogeosciences*, 11, 2027–2054, <https://doi.org/10.5194/bg-11-2027-2014>, 2014.
- Thompson, S. L. and Pollard, D.: A global climate model (GENESIS) with a land-surface transfer scheme (LSX). Part I: present climate simulation, *J. Climate*, 8, 732–761, [https://doi.org/10.1175/1520-0442\(1995\)008<0732:AGCMWA>2.0.CO;2](https://doi.org/10.1175/1520-0442(1995)008<0732:AGCMWA>2.0.CO;2), 1995.
- Torello-Raventos, M., Feldpausch, T., Veenendaal, E., Schrodte, F., Saiz, G., Domingues, T., Djagbletey, G., Ford, A., Kemp, J., Marimon, B., Hur Marimon Junior, B., Lenza, E., Ratter, J., Maracahipes, L., Sasaki, D., Sonké, B., Zapfack, L., Taedoumg, H., Villarreal, D., Schwarz, M., Quesada, C., Yoko Ishida, F., Nardoto, G., Affum-Baffoe, K., Arroyo, L., Bowman,

- D., Compaore, H., Davies, K., Diallo, A., Fyllas, N., Gilpin, M., Hien, F., Johnson, M., Killeen, T., Metcalfe, D., Miranda, H., Steininger, M., Thomson, J., Sykora, K., Mougín, E., Hiernaux, P., Bird, M., Grace, J., Lewis, S., Phillips, O., and Lloyd, J.: On the delineation of tropical vegetation types with an emphasis on forest/savanna transitions, *Plant Ecol. Divers.*, 6, 101–137, <https://doi.org/10.1080/17550874.2012.762812>, 2013.
- Valadão, M. B. X., Marimon-Junior, B. H., Oliveira, B., Lúcio, N. W., Souza, M. G. R., and Marimon, B. S.: AGB hyperdynamic as a key modulator of forest self-maintenance in dystrophic soil at Amazonia-Cerrado transition, *Sci. For.* 44, 475–485, 2016.
- Veenendaal, E. M., Torello-Raventos, M., Feldpausch, T. R., Domingues, T. F., Gerard, F., Schrodte, F., Saiz, G., Quesada, C. A., Djangbletey, G., Ford, A., Kemp, J., Marimon, B. S., Marimon-Junior, B. H., Lenza, E., Ratter, J. A., Maracahipes, L., Sasaki, D., Sonké, B., Zapfack, L., Villarroya, D., Schwarz, M., Yoko Ishida, F., Gilpin, M., Nardoto, G. B., Affum-Baffoe, K., Arroyo, L., Bloomfield, K., Ceca, G., Compaore, H., Davies, K., Diallo, A., Fyllas, N. M., Gignoux, J., Hien, F., Johnson, M., Mougín, E., Hiernaux, P., Killeen, T., Metcalfe, D., Miranda, H. S., Steininger, M., Sykora, K., Bird, M. I., Grace, J., Lewis, S., Phillips, O. L., and Lloyd, J.: Structural, physiognomic and above ground biomass variation in savanna–forest transition zones on three continents – how different are co-occurring savanna and forest formations?, *Biogeosciences*, 12, 2927–2951, <https://doi.org/10.5194/bg-12-2927-2015>, 2015.
- Verberne, E. L. J., Hassink, J., De Willigen, P., Groot, J. J. R., and Van Veen, J. A.: Modelling organic matter dynamics in different soils, *Netherlands J. Agric. Sci.*, 38, 221–238, 1990.
- Vourlitis, G. L., de Lobo, F. A., Lawrence, S., de Lucena, I. C., Pinto, O. B., Dalmagro, H. J., Ortiz, C. E., and de Nogueira, J. S.: Variations in Stand Structure and Diversity along a Soil Fertility Gradient in a Brazilian Savanna (Cerrado) in Southern Mato Grosso, *Soil Sci. Soc. Am. J.*, 77, 1370–1379, <https://doi.org/10.2136/sssaj2012.0336>, 2013.
- Wang, S., Huang, J., He, Y., and Guan, Y.: Combined effects of the Pacific Decadal Oscillation and El Niño–Southern Oscillation on Global Land Dry–Wet Changes, *Sci. Rep.*, 4, 6651, <https://doi.org/10.1038/srep06651>, 2014.
- Yang, X., Post, W. M., Thornton, P. E., and Jain, A.: The distribution of soil phosphorus for global biogeochemical modeling, *Biogeosciences*, 10, 2525–2537, <https://doi.org/10.5194/bg-10-2525-2013>, 2013.
- Yang, X., Thornton, P. E., Ricciuto, D. M., and Post, W. M.: The role of phosphorus dynamics in tropical forests – a modeling study using CLM-CNP, *Biogeosciences*, 11, 1667–1681, <https://doi.org/10.5194/bg-11-1667-2014>, 2014.